PHYSICA Ⓒ

Density of states in high-T_c superconductors

Suresh V. Vettoor and V.M. Nandakumaran

Department of Physics, Cochin University of Science & Technology, Cochin-22, India

The density of states and the low temperature specific heat of high-T_c superconductors are calculated in a functional integral formalism using the slave boson technique. The manybody calculation in a saddle point approximation shows that the low energy sector is dominated by a single band. The calculated values of density of states are in good agreement with experimental results.

1. Introduction

High temperature superconductivity in ceramic oxides raises serious questions regarding the mechanism of normal and superconducting state properties of these systems. Ever since the discovery [1], various theoretical models have been suggested and different mechanisms ranging from conventional weak coupling BCS-like to novel strong coupling formulations have been proposed [2–4]. But still there is no general consensus on the relevant parameter regime and the mechanism of superconductivity in these systems.

It is believed that the essential physics of normal and superconducting states reside in the Cu–O planar subsystem which is common to the copper oxide superconductors.

Many theoretical models begin with a two-dimensional extended Hubbard model or Anderson lattice model with a strong on-site repulsive interaction [5–7]. The introduction of nearest neighbour repulsion in the extended Hubbard model [8] emphasizes the relevance of charge degrees of freedom. In the t–J models and RVB theories the low energy sector of the problem is dominated by the spin degrees of freedom [9,10].

In this paper we analyze the extended model without nearest neighbour repulsion, but with a direct oxygen–oxygen hopping between the Pσ orbitals which brings to the scene, in addition to the spin degrees of freedom, the charge degrees of freedom.

These models have been previously studied using a mean field scheme [11,12]. We studied this strongly correlated problem using a slave boson [13] functional integral formalism [14] adopting a uniform saddle point approximation in the complex variables.

Photo emission studies show that the copper on-site repulsion is the largest energy scale in the problem. At half filling, the materials are antiferromagnetically spin ordered insulators. The proximity to being a magnetic insulator makes strong correlation relevant to the doped case.

Here we consider a model, in which the on-site repulsion imposes a double occupancy constraint on the copper $3d_{x^2-y^2}$ orbital. We study this using a large N expansion technique which is nonperturbative in the coupling constants. The study is restricted to the mean field theory ($N=\infty$). The partition function and the free energy are derived in section 2. The expressions for the specific heat and the density of states have been derived in section 3. The numerical computations are presented in section 4. The conclusions concerning the renormalized energy bands and the comparison with experiments are also discussed in section 4.

2. The model

The model we consider in this paper has three essential bands. As a consequence of the oxygen ligand environment the copper 3d degeneracy is lifted and

the orbital which is closer to the Fermi energy is the copper $3d_{x^2-y^2}$ orbital. The relevant oxygen orbitals are the p_σ orbitals of x and y symmetry.

The Hamiltonian for the system can be written as

$$H = \epsilon_d \sum_{i,\sigma} d^\dagger_{i\sigma} d_{i\sigma} + \epsilon_p/2 \sum_{i,\eta_1,\sigma} p^\dagger_{i+\eta_1,\sigma}(x) p_{i+\eta_1,\sigma}(x)$$

$$+ \epsilon_p/2 \sum_{i,\eta_2,\sigma} p^\dagger_{i+\eta_2,\sigma}(y) p_{i+\eta_2,\sigma}(y)$$

$$+ t_{pd} \sum_{i,\eta_1,\sigma} d^\dagger_{i\sigma} p_{i+\eta_1,\sigma}(x)$$

$$+ t_{pd} \sum_{i,\eta_2,\sigma} d^\dagger_{i\sigma} p_{i+\eta_2,\sigma}(y) + \text{h.c.}$$

$$+ U/2 \sum_{\substack{i,\sigma,\sigma' \\ (\sigma \neq \sigma')}} d^\dagger_{i\sigma} d_{i\sigma} d^\dagger_{i\sigma'} d_{i\sigma'}$$

$$+ t_p \sum_{\substack{\eta_1,\eta_2 \\ i,\sigma}} p^\dagger_{i+\eta_1,\sigma}(x) p_{i+\eta_2,\sigma}(y)$$

$$+ t_p \sum_{\substack{\eta_1,\eta_2 \\ i,\sigma}} p^\dagger_{i+\eta_2,\sigma}(y) p_{i+\eta_1,\sigma}(x) , \quad (1)$$

where η_1 takes values a_x and $-a_x$ and η_2 takes values a_y and $-a_y$. The scale is so chosen that their magnitudes are 1. ϵ_p and ϵ_d are the unrenormalized energy levels. They include the chemical potential. $d^\dagger_{i\sigma}$ and $d_{i\sigma}$ are the Fermi creation and annihilation operators for holes in the filled copper $3d_{x^2-y^2}$ orbital. $p^\dagger_{i+\eta_1,\sigma}(x)$ and $p_{i+\eta_1,\sigma}(x)$ are the creation and annihilation operators for holes in a p_σ orbital next to the ith planar copper atom. Similarly the other p operators correspond to the oxygen p_σ orbital with y symmetry. In the low energy sector which is relevant at low temperatures, the large U limit imposes constraints on the hole dynamics.

Using a large N slave boson technique with $b^\dagger_i$ and b_i as the slave boson operators, the Hamiltonian takes the form

$$H = \epsilon_d \sum_{i,\sigma} d^\dagger_{i\sigma} d_{i\sigma} + \epsilon_p/2 \sum_{i,\eta_1,\sigma} p^\dagger_{i+\eta_1,\sigma}(x) p_{i+\eta_1,\sigma}(x)$$

$$+ \epsilon_p/2 \sum p^\dagger_{i+\eta_2,\sigma}(y) p_{i+\eta_2,\sigma}(y)$$

$$+ (t_{pd}/\sqrt{N}) \sum_{\eta_1,\sigma} b_i d^\dagger_{i\sigma} p_{i+\eta_1,\sigma}(x)$$

$$+ t_{pd}/\sqrt{N} \sum_{\substack{i,\sigma \\ \eta_2}} b_i d^\dagger_{i\sigma} p_{i+\eta_2,\sigma}(y) + (\text{h.c.})$$

$$+ t_p/\sqrt{N} \sum_{\substack{i,\sigma \\ \eta_1,\eta_2}} p^\dagger_{i+\eta_1,\sigma}(x) p_{i+\eta_2,\sigma}(y)$$

$$+ t_p/\sqrt{N} \sum_{\substack{i,\sigma \\ \eta_1,\eta_2}} p^\dagger_{i+\eta_2,\sigma}(y) p_{i+\eta_1,\sigma}(x)$$

$$+ i \sum_i \lambda_i \left\{ b^\dagger_i b_i + \sum_\sigma d^\dagger_{i\sigma} d_{i\sigma} - q_0 N_0 \right\} . \quad (2)$$

The partition function for the model in the functional integral formalism takes the form

$$Z = \int D[d] D[p] D[b] d\lambda_i e^{-S} , \quad (3)$$

where

$$S = \int_0^\beta L \, d\tau \quad (4)$$

$$L = \sum_i \left[\sum_\sigma \bar{d}_{i\sigma} \frac{\partial}{\partial \tau} d_{i\sigma} + \sum_{\sigma,\eta_1} \bar{p}_{i+\eta_1,\sigma}(x) \frac{\partial}{\partial \tau} p_{i+\eta_1,\sigma}(x) \right.$$

$$\left. + \sum_{\sigma,\eta_2} \bar{p}_{i+\eta_2,\sigma}(y) \frac{\partial}{\partial \tau} p_{i+\eta_2,\sigma}(y) \right]$$

$$+ i \sum_i \lambda_i [\bar{b}_i b_i - q_0 N] + H , \quad (5)$$

where

$$H = \sum_{i,\sigma} \bar{d}_{i\sigma} d_{i\sigma}(\epsilon_d + i\lambda_i) + \sum_{\substack{i \\ \sigma,\eta_1}} \bar{p}_{i+\eta_1,\sigma}(x) p_{i+\eta_1,\sigma}(x) \epsilon_p$$

$$+ \sum_{\substack{i \\ \sigma,\eta_2}} \bar{p}_{i+\eta_2,\sigma}(y) p_{i+\eta_2,\sigma}(y) \epsilon_p$$

$$+ (t_{pd}/\sqrt{N}) \sum_{\substack{i \\ \sigma,\eta_1}} \bar{d}_{i\sigma} p_{i+\eta_1,\sigma}(x) b_i$$

$$+ (t_{pd}/\sqrt{N}) \sum \bar{d}_{i\sigma} p_{i+\eta_2,\sigma}(y) b_i + (\text{h.c.})$$

$$+ (t_p/\sqrt{N}) \sum_{\substack{i,\sigma \\ \eta_1,\eta_2}} [\bar{p}_{i+\eta_1,\sigma}(x) p_{i+\eta_2,\sigma}(y)$$

$$+ \bar{p}_{i+\eta_2,\sigma}(y) p_{i+\eta_1,\sigma}(x)] , \quad (6)$$

where $\bar{d}_{i\sigma}$, $d_{i\sigma}$, $\bar{p}_{i+\eta_1,\sigma}(x)$, $p_{i+\eta_1,\sigma}(x)$, $\bar{p}_{i+\eta_2,\sigma}(y)$, $p_{i+\eta_2,\sigma}(y)$ are Grassmann variables corresponding to Fermi creation and annihilation operators.

We make a uniform saddle point approximation in the slave boson variables and Lagrange multiplier variables. We denote them as λ and b. The functional integrals over the Grassmann variables are per-

formed after converting the Grassmann variables from real space to momentum space and from imaginary time to imaginary frequency representation.

The partition function then becomes

$$Z = e^{-\beta F},\tag{7}$$

where the free energy is given for real degeneracy of σ which is 2:

$$F = -(1/\beta)\sum_{k,\sigma}[\ln(1+e^{-\beta\bar{\epsilon}_d})$$

$$+2\ln(1+e^{-\beta\epsilon_p})]$$

$$-(1/\beta)\sum_{n,k,\sigma}[2\ln(G(\epsilon_p,i\omega_n))$$

$$+\ln(A(x)A(y)-B)]$$

$$+N_s\lambda b^2 - N_s\lambda,\tag{8}$$

where N_s is the number of copper sites in the planar subsystem,

$$G(\epsilon_p, i\omega_n) = (\epsilon_p - i\omega_n)^{-1},\tag{9}$$

$i\omega_n$ are the Matsubara frequencies

$$i\omega_n = (2n+1)(i\pi/\beta)\tag{10}$$

and n varies from $-\alpha$ to α; and we have

$$\bar{\epsilon}_d = \epsilon_d + \lambda,\tag{11}$$

$A(x)$

$$= \frac{((\epsilon_p - i\omega_n)(\bar{\epsilon}_d - i\omega_n) - 4t_{pd}^2\sin(k_x/2))}{(\bar{\epsilon}_d - i\omega_n)},\tag{12}$$

$A(y)$

$$= [(\epsilon_p - i\omega_n)(\bar{\epsilon}_d - i\omega_n)$$

$$-4t_{pd}^2\sin^2(k_y/2)](\bar{\epsilon}_d - i\omega_n)^{-1},\tag{13}$$

and

$$B = 16(t_p - t_{pd}^2 b^2(\bar{\epsilon}_d - i\omega_n)^{-1})^2$$

$$\times \sin^2(k_x/2)\sin^2(k_y/2).\tag{14}$$

The saddle point values are determined by

$$\frac{\partial F}{\partial\lambda} = 0 \quad\text{and}\quad \frac{\partial F}{\partial b^2} = 0.\tag{15}$$

We can write

$$A(x)A(y) - B = \frac{P(i\omega_n)}{(\bar{\epsilon}_d - i\omega_n)^2},\tag{16}$$

where

$$P(i\omega_n) = a_0(i\omega_n)^4 - 2a_1(i\omega_n)^3 + a_2(i\omega_n)^2$$

$$+a_3(i\omega_n) + a_4,\tag{17}$$

and a_0, a_1, a_2, a_3, a_4 stand for

$$a_0 = 1,\tag{18}$$

$$a_1 = \bar{\epsilon}_d + \epsilon_p,\tag{19}$$

$$a_2 = a_1^2 + \epsilon_p\bar{\epsilon}_d - 4t_{pd}^2 b^2\gamma_1 - 16t_p^2\gamma_2,\tag{20}$$

$$a_3 = (4t_{pd}^2 b^2\gamma_1 - 2\bar{\epsilon}_d\epsilon_p)a_1$$

$$+32(t_p^2\bar{\epsilon}_d - t_{pd}^2 t_p b^2)\gamma_2,\tag{21}$$

and

$$a_4 = \bar{\epsilon}_d\epsilon_p - 4t_{pd}^2\bar{\epsilon}_d\epsilon_p b^2\gamma_1$$

$$+16(2t_{pd}^2 b^2 - t_p\bar{\epsilon}_d)t_p\bar{\epsilon}_d\gamma_2,\tag{22}$$

where γ_1 and γ_2 are

$$\gamma_1 = \sin^2(k_x/2) + \sin^2(k_y/2),\tag{23}$$

$$\gamma_2 = \sin^2(k_x/2)\sin^2(k_y/2).\tag{24}$$

$P(i\omega_n)$ can be written as

$$P(i\omega_n) = \prod_{j=1}^{4}(E(j) - i\omega_n)\tag{25}$$

where $E(j)$ are the roots of the polynomial $P(i\omega_n)$. When frequency sums are performed after simplifications the expression for the free energy becomes

$$F = \sum_{k,\sigma}(1/\beta)\left[\ln\left(1+e^{-\beta\bar{\epsilon}_d}\right) - \sum_{j=1}^{4}\ln\left(1+e^{-\beta E(j)}\right)\right]$$

$$+N_s\lambda b^2 - N_s\lambda.\tag{26}$$

3. The electronic specific heat capacity and density of states

The electronic specific heat capacity is given by the expression

$$C_v = -T\frac{\partial^2 F}{\partial T^2},\tag{27}$$

where T is the temperature.

At the low temperatures of interest to us, we can set $\beta \to \infty$. The limit is applied after taking the derivatives. We can write

$$\frac{\partial^2 F}{\partial T^2}$$

$$= \sum_{k,\sigma} \bar{\epsilon}_d^2 k_B^2 \beta^3 \frac{e^{\beta \bar{\epsilon}_d}}{(e^{\beta \bar{\epsilon}_d}+1)^2}$$

$$- \sum_{k,j,\sigma} k_B^2 \beta^3 \frac{E^2(j) e^{\beta E(j)}}{(e^{\beta E(j)}+1)^2} . \tag{28}$$

The summations over k can be replaced by integration. When this is done the contribution of the first term vanishes in the $\beta \to \infty$ limit since the integrand is independent of the integration variables. The second term is simplified and on substitution in eq. (27) yields the specific heat capacity per copper site in the planar structures as

$$C_v = \frac{2\pi k_B^2 T}{3}$$

$$\times \left[2/\pi \int_0^\pi dk_y \sum_{j=1}^4 \left(\frac{\partial E(j)}{\partial k_y} \bigg|_{E(j)=0} \right)^{-1} \right], \tag{29}$$

where the quantity enclosed inside the square brackets can be identified as the density of states at the Fermi surface.

4. Numerical results and conclusions

The saddle point values λ and b^2 are determined numerically using eqs. (15) for β in the ∞ limit. When the numerical integrations over k_x and k_y are performed, at each integration step eq. (17) is numerically solved to determine the energy values $E(j)$. Using the saddle point values, the density of states calculation is carried out. The variation of density of states with doping is plotted. The chemical potentials are so chosen that the average number of particles is given by

$$N_s(1+\delta) = -\frac{\partial F}{\partial \mu}, \tag{30}$$

where δ is the doping concentration and μ is the chemical potential.

The computations are carried out for two sets of parameter values

(1) $t_p = -0.5$ eV, $t_{pd} = -1.5$ eV, $\epsilon_p = -4.0 t_p$ eV, $\epsilon_d = (\epsilon_p - 1.8)$ eV;

(2) $t_p = -0.1$ eV, $t_{pd} = -1.5$ eV, $\epsilon_p = -4.0 t_p$ eV, $\epsilon_d = (\epsilon_p - 1.8)$ eV.

The variation of the density of states with δ is shown in fig. 1. For very small values of δ (close to the half filled case) the saddle point values show large deviations. The corresponding density of states also shows an increase. When δ is very small the saddle point values become a poor approximation for the functional integral in view of the constraint in the problem. Therefore we are not including the limiting half filled case in the discussion. In the other domain the pattern of the variation of the density of states
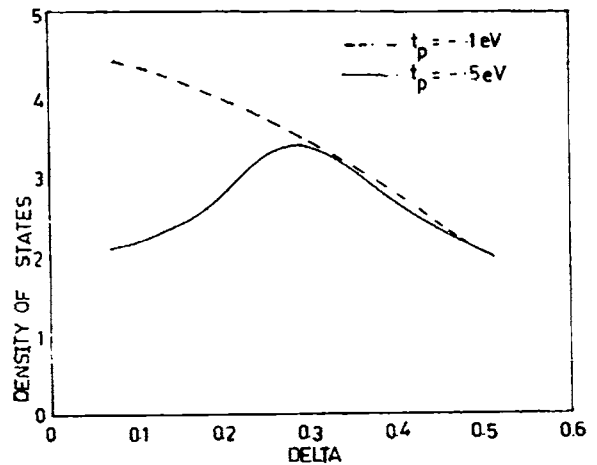

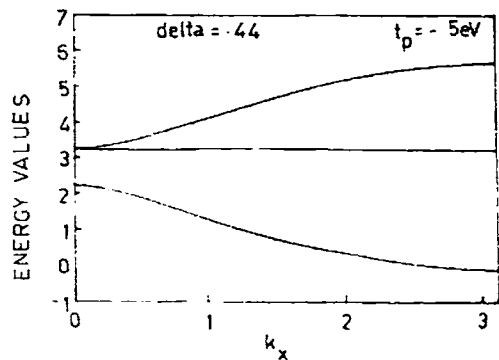Fig. 1. Density of states vs. doping for $t_p = -0.5$ eV and $t_p = -0.1$ eV.

Fig. 2. Energy values vs. k_x in the range 0 to π for $k_y = 0$.

is similar to that of ref. [11]. The renormalized energy bands are shown in figs. 2 and 3. The two-dimensional analogue of the Fermi surface is shown in fig. 4. The calculated values of density of states are in good agreement with the values deduced by Grilli et al. [11] from susceptibility measurements [15]. The renormalized energy bands in figs. 2 and 3 show
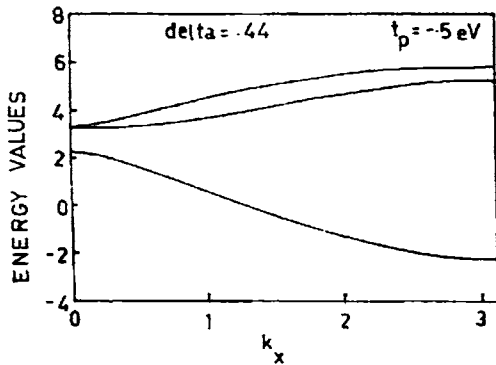
that in the low energy domain the physics is governed by a single band as has been advocated by Anderson [16].

We have shown that even for moderately large t_p values and for the parameter regime considered in this paper the effective one band description holds. The calculated values of the density of states are in good agreement with estimations from experiments.

Fig. 3. Energy values vs. k_x in the range 0 to π for $k_y = k_x$.
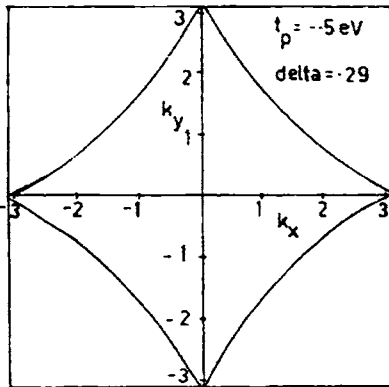
Fig. 4. Contour in the two-dimensional k space where the energy value crosses zero.

References

[1] G. Bednorz and A. Müller, Z. Phys. B 64 (1986) 189.
[2] P.W. Anderson, Science 235 (1987) 1196.
[3] V.J. Emery, Phys. Rev. Lett. 58 (1987) 2794.
[4] R.B. Laughlin, Science 242 (1988) 525.
[5] C.M. Varma, P.B. Littlewood, S. Schmitt-Rink and E. Abrahams, Solid State Commun. 62 (1987) 681.
[6] G. Kotliar, P.A. Lee and N. Reed, Physica C 153-155 (1988) 538.
[7] D.M. Newns, M. Rasoh and P.C. Pattnaik, Phys. Rev. B 38 (1988) 6513.
[8] S. Schmitt-Rink, C.M. Varma and A.E. Ruckenstein, Phys. Rev. Lett. 60 (1988) 2793.
[9] F.C. Shang and T.M. Rice, Phys. Rev. B 37 (1988) 3759.
[10] G. Baskaran, Z. Zou and P.W. Anderson, Solid State Commun. 63 (1987) 973.
[11] M. Grilli, B.G. Kotliar and A.J. Millis, Phys. Rev. B 42 (1990) 329.
[12] C.A. Balaseiro, M. Avignon, A.G. Rojo and B. Alascio, Phys. Rev. Lett. 62 (1989) 2624.
[13] S.E. Barnes, J. Phys. F 6 (1976) 1375.
[14] J.W. Negele and H. Orland, Quantum Many Particle Systems (Addison-Wesley, Reading, MA, 1988).
[15] L.F. Schneemeyer, J.V. Waszczak, E.A. Reitman and R.J. Cava, Phys. Rev. B 35 (1987) 8421.
[16] P.W. Anderson, Int. J. Mod. Phys. B 4 (1990) 181.